ELSEVIER

Biophysical Chemistry 119 (2006) 186 – 195

Biophysical Chemistry

http://www.elsevier.com/locate/biophyschem

Molecular crowding effects of linear polymers in protein solutions

Donald J. Winzor [a,*], Peter R. Wills [b]

[a] Department of Biochemistry, School of Molecular and Microbial Sciences, University of Queensland, Brisbane, Queensland 4072, Australia
[b] Department of Physics, The University of Auckland, Private Bag 92019, Auckland, New Zealand

Received 31 May 2005; received in revised form 3 August 2005; accepted 3 August 2005
Available online 29 August 2005

Abstract

Measurement of protein–polymer second virial coefficients (B_{AP}) by sedimentation equilibrium studies of carbonic anhydrase and cytochrome *c* in the presence of dextrans (T10–T80) has revealed an inverse dependence of B_{AP} upon dextran molecular mass that conforms well with the behaviour predicted for the excluded-volume interaction between a spherical protein solute *A* and a random-flight representation of the polymeric cosolute *P*. That model of the protein–polymer interaction is also shown to provide a reasonable description of published gel chromatographic and equilibrium dialysis data on the effect of polymer molecular mass on B_{AP} for human serum albumin in the presence of polyethylene glycols, a contrary finding from analysis of albumin solubility measurements being rejected on theoretical grounds. Inverse dependence upon polymer chainlength is also the predicted excluded-volume effect on the strength of several types of macromolecular equilibria—protein isomerization, protein dimerization, and 1 : 1 complex formation between dissimilar protein reactants. It is therefore concluded that published experimental observations of the reverse dependence, preferential reaction enhancement within DNA replication complexes by larger polyethylene glycols, must reflect the consequences of cosolute chemical interactions that outweigh those of thermodynamic nonideality arising from excluded-volume effects.

Keywords: Protein–polymer virial coefficients; Thermodynamic nonideality; Polymer molecular-crowding effects; Dextrans; Polyethylene glycols

1. Introduction

The potential consequences of thermodynamic nonideality arising from molecular crowding by inert cosolutes have been subjected to considerable scrutiny because of their relevance to the concentrated physiological environment [1–3]. For cosolutes that exhibit colligative properties commensurate with those predicted on the statistical–mechanical basis of excluded volume for rigid spheres, the effectiveness of molecular crowding varies inversely with molecular mass when cosolute concentration is expressed on a weight basis. Advantage has been taken of this prediction [4,5] by the use of small cosolutes in studies designed to distinguish between pre-existence and substrate-induction of enzyme isomerizations [6–10].

Far more popular has been the use of linear polymers such as polyethylene glycol and dextran to effect the displacement of protein equilibria by molecular crowding. For these crowding agents, however, the dependence of the effect is less clear. Experimental studies of the effect of polyethylene glycol on interactions within DNA replication complexes [11–14] have indicated a progressive increase in the binding constant with increasing size of the space-filling polymer. On the other hand, theoretical studies have predicted independence of the extent of interaction enhancement upon polymer chainlength for long rod [15] and flexible-segment [16] models of the cosolute. Detailed consideration remains to be given to the effect of polymer chainlength upon excluded volume effects for a more realistic model involving representation of the cosolute as an effective Brownian walk with specified root-mean-square end-to-end length l_P [17].

The purpose of this investigation is two-fold. Results from studies of the effects of polyethylene glycol and

* Corresponding author. Tel.: +61 7 3870 0243; fax: +61 7 3365 4699.
E-mail address: d.winzor@uq.edu.au (D.J. Winzor).

0301-4622/$ - see front matter © 2005 Elsevier B.V. All rights reserved.
doi:10.1016/j.bpc.2005.08.001

dextran on the thermodynamic activity of individual proteins are first checked for conformity with the behaviour predicted by the Jansons–Phillips model of the protein–polymer excluded-volume interaction [17]. Comparable inverse dependence of the excluded-volume effect upon cosolute chainlength is also the prediction for several types of macromolecular interaction—protein isomerization, reversible protein dimerization, and reversible complex formation between protein reactants differing considerably in size. We therefore conclude that the greater enhancement of interactions within DNA replication complexes by longer polyethylene glycol chains [11–14] must reflect the consequences of preferential chemical interactions of cosolute with complexes that outweigh those emanating from excluded volume effects.

2. Experimental

2.1. Preparation of protein–polymer mixtures

Bovine erythrocyte carbonic anhydrase and bovine heart cytochrome *c* were commercial preparations supplied by Sigma Chemical Co., St. Louis, MO. Dextrans T10, T20, T40, T80 were obtained from Pharmacia Fine Chemicals, Uppsala, Sweden. The proteins were dissolved directly in phosphate buffer (0.04 M NaH_2PO_4–0.04 M Na_2HPO_4), pH 6.8, *I* 0.16 M, and dialyzed against more of the same buffer, after which concentrations of these stock protein solutions were determined spectrophotometrically at 280 nm on the basis of absorption coefficients ($A^{1\%}_{1\,cm}$) of 18.0 and 18.4 for carbonic anhydrase [18] and cytochrome *c* [19], respectively. Solutions for sedimentation experiments were then prepared by dilution of these stock protein solutions either with buffer or with polymer-supplemented buffer to yield solutions with the required initial composition (protein concentration approx. 0.2 mg/ml, dextran concentrations in the range 1 mg/ml (for T80) to 10 mg/ml (for T10).

2.2. Determination of the second virial coefficient for protein–polymer interaction

Second virial coefficients (B_{AP}) for the excluded volume interactions of carbonic anhydrase and cytochrome *c* (species *A*) with the various dextrans (polymeric cosolute *P*) were determined by a variant of the sedimentation equilibrium procedure described previously [20]. Solutions of protein alone and of protein–polymer mixtures (A_{280}=0.4–0.5 for both solutions) were subjected to simultaneous sedimentation equilibrium in a Beckman XL-I ultracentrifuge operated at 14,000 rpm and 20 °C. Spectrophotometric scans at 280 nm were used to deduce the equilibrium protein distributions, whereas the Rayleigh optical system was used to monitor the total concentration distribution. The Rayleigh distribution for dextran was then determined by subtracting the protein contribution to the Rayleigh distribution based on the conversion factor reported by Voelker [21] (1 mg/ml≡3.33 fringes). Concentration distributions for dextran (mg/ml) measured relative to that at a reference radial position r_F close to the meniscus were then obtained by means of the expression [22]

$$c_P(r) - c_P(r_F) = [J_P(r) - J_P(r_F)]/(17.5\mathrm{d}n/\mathrm{d}c_P) \quad (1)$$

where $[J_P(r)-J_P(r_F)]$ refers to the number of fringes between radial distances *r* and r_F for polymer with specific refractive index increment $\mathrm{d}n/\mathrm{d}c_P$: a value of 0.150 ml/g was used for dextran [23].

At sedimentation equilibrium the molar thermodynamic activity of the protein, $z_A(r)$, at radial distance *r* is related to that, $z_A(r_F)$, at a reference radial position r_F by the expressions [24]

$$z_A(r) = z_A(r_F)\psi_A(r) \quad (2a)$$

$$\psi_A(r) = \exp\left[M_A(1-\bar{\nu}_A\rho_S)\omega^2\left(r^2 - r_F^2\right)/(2RT)\right] \quad (2b)$$

in an experiment conducted at angular velocity ω and absolute temperature *T*: $\bar{\nu}_A$ is the partial specific volume of the protein, ρ_S the buffer density, and *R* the universal gas constant. Because the experiment on protein alone is being conducted under conditions approaching thermodynamic ideality, the absorbance distribution may be analyzed in terms of Eqs. (2a,b) with $A_{280}(r)$ substituted for $z_A(r)$ to determine the magnitude of $M_A(1-\bar{\nu}_A\rho_S)\omega^2/(2RT)$.

Although Eqs. (2a,b) also describe the activity distribution in the simultaneous experiment on the protein–dextran mixture, they do not describe the radial dependence of the protein concentration (or A_{280}). Analysis of the molar protein concentration distribution [$C_A(r)$ as a function of *r*] in terms of Eqs. (2a,b) requires introduction of the relationship

$$z_A(r) \approx C_A(r)\exp[B_{AP}C_P(r)] \quad (3)$$

in which B_{AP} is the second virial coefficient describing the excluded-volume interaction between protein and polymer, present at molar concentration $C_P(r)$. Combination of Eqs. (2a,b) and (3) leads to the conclusion that

$$A_{280}(r)/\psi_A(r) = A_{280}(r_F)\exp\{-(B_{AP}/M_P)[c_P(r) - c_P(r_F)]\} \quad (4)$$

where the molar cosolute concentration has been replaced by its weight-concentration counterpart, c_P, to allow expression of the virial coefficient on a litre/gram rather than a litre/mol basis. This specific protein–cosolute virial coefficient, B_{AP}/M_P, is thus conveniently obtained from the logarithmic transform of Eq. (4), namely

$$\ln[A_{280}(r)/\psi_A(r)] = \ln A_{280}(r_F) - (B_{AP}/M_P)[c_P(r) - c_P(r_F)] \quad (5)$$

as the slope $(-B_{AP}/M_P)$ of the dependence of ln $[A_{280}(r)/\psi_A(r)]$ upon $[c_P(r)-c_P(r_F)]$. In that regard the magnitude

of $M_A(1-\bar{\nu}_A\rho_S)\omega^2/(2RT)$ required for the evaluation of $\psi_A(r)$ has already been obtained from the parallel sedimentation equilibrium experiment on protein alone.

2.3. Parameters for the statistical mechanical representation of B_{AP}

For an uncharged polymer chain the second virial coefficient for protein–polymer excluded-volume interaction, B_{AP}, is simply the covolume—the volume from which the polymer and protein molecules mutually exclude each other. As a first approximation a globular protein may be represented as an impenetrable sphere with radius R_A [15–17], whereas the extended form of polymer chains is more appropriately represented as an effective Brownian walk of specified root-mean-square end-to-end length l_P [17]. The covolume for this combination is given by

$$B_{AP} = N\left[(2\pi/3)R_A l_P^2 + 4(2\pi/3)^{1/2}R_A^2 l_P + (4\pi/3)R_A^3\right]. \quad (6)$$

For a linear polymer the relationship $l_P^2=6R_g^2$ allows a magnitude to be assigned to the root-mean-square end-to-end length on the basis of the radius of gyration (R_g), an experimentally determinable parameter that emanates from static light-scattering studies. As noted previously [20], such consideration of the dependence of R_g upon molecular mass for polyethylene glycol [25] leads to the expression $l_P=(0.006M_P)^{1/2}$ nm, with M_P measured in Da. The corresponding relationship $l_P=0.118M_P^{0.46}$ nm is deduced from the dependence of R_g upon weight-average molecular mass reported [26] for Pharmacia dextrans. Protein radii, R_A, have been taken as 2.43 nm for carbonic anhydrase [27] and 1.65 nm for cytochrome *c* [28].

There are also literature studies in which the polymer has been described in terms of a rigid impenetrable sphere characterized by the viscosity-average radius R_P. For this model the counterpart of Eq. (6) is simply

$$B_{AP} = (4\pi N/3)(R_A + R_P)^3. \quad (7)$$

In present applications of Eq. (7) the values of R_P have been calculated from the expressions $R_P=0.0292M_P^{0.5}$ nm ($200 \le M_P \le 8000$ Da) and $R_P=0.0126M_P^{0.593}$ nm ($M_P \ge 10{,}000$ Da), in accordance with the procedure used by Atha and Ingham [29]. Those for dextrans have been calculated as $R_P=0.0271M_P^{0.498}$ nm [30].

3. Results and discussion

The realization that effects of linear polymers on protein properties could be rationalized qualitatively on the statistical–mechanical basis of excluded volume [15,31,32] has prompted many considerations of the extent to which this molecular crowding effect might describe quantitatively the observed thermodynamic nonideality of a protein in the presence of macromolecular cosolutes [1–3,15,20,33,34]. Various models have been used to account for thermodynamic nonideality arising from protein–polymer interactions. Inasmuch as the protein has invariably been regarded as an impenetrable sphere, the differences reside in the model used to represent the polymer. The concept of impenetrability is retained in the simpler models of the polymer as either a sphere or a long rod [15]. Of models of that take into account segment flexibility of the polymer [16,17,35], the most realistic is that based on its representation as an effective Brownian walk with specified root-mean-square end-to-end length l_P [17].

Although experimental protein–polymer virial coefficients were shown to conform with the Jansons–Phillips model [17] in a previous investigation [20], that demonstration of the adequacy of the theory entailed use of the dependence of B_{AP}/M_P upon R_A to obtain an effective root-mean-square end-to-end length l_P for single polymer samples (PEG-20000 and Dextran T70). We therefore commence this investigation with an examination of the dependence of the protein–polymer virial coefficient upon polymer size M_P for dextrans.

3.1. Variation of the protein–polymer virial coefficient with dextran molecular mass

Our previous investigation of protein–polymer interactions [20] introduced a sedimentation equilibrium technique that yielded B_{AP}/M_P from a direct comparison of the protein distributions in simultaneous runs on protein alone and protein supplemented with cosolute (PEG-20000 or Dextran T70). Specifically, the method entailed use of the expression

$$\ln\{A_{280}(r)/[A_{280}(r)]_P\} = \ln\{A_{280}(r_F)/[A_{280}(r_F)]_P\} + (B_{AP}/M_P)[c_P(r) - c_P(r_F)] \quad (8)$$

where the P subscript signifies an absorbance for the polymer-supplemented sample. In this very simple analysis the virial coefficient is thus obtained from the ratio of protein absorbances (concentrations) at the same radial distance in the two cells as a function of $[c_P(r)-c_P(r_F)]$, which is also a direct measurement. However, that method reflects its development in the era of the Beckman model E ultracentrifuge, when selection of a common radial distance in the two cells was readily effected because of operator involvement in the manual measurement of photographically recorded distributions.

Automated measurement of the equilibrium distributions has certainly eased the tedium of analytical ultracentrifugation, but renders less efficient the above analysis because of the requirement for absorbance and fringe readings at identical radial distances in the two distributions being compared. In that regard the much closer spacing of Rayleigh fringe measurements allows fulfillment of the

requirement for obtaining $[A_{280}(r)]_P$ and $[J(r)]_P$ at essentially identical values of radial distance r. To avoid the necessity of rejecting much of those data for want of a corresponding measurement of $A_{280}(r)$ in the absence of polymer, that distribution has now been analyzed in terms of Eqs. (2a) and (2b) to allow the substitution in Eq. (8) of $A_{280}(r_F)\psi_A(r)$ for $A_{280}(r)$ at all radial distances pertinent to the $[A_{280}(r)]_P$ measurements. Such action leads to Eq. (5), where the subscript P has been removed on the grounds that only measurements in the presence of polymeric cosolute are involved. This modified analysis of sedimentation equilibrium distributions is illustrated for the carbonic anhydrase–Dextran T20 system in Fig. 1, where the results are plotted in the manner suggested by Eq. (5). Linear-least-squares analysis leads to best-fit values of −3.07 (±0.02) and 35 (±4) ml/g for ln $A_{280}(r_F)$ and B_{AP}/M_P, respectively.

The variation of B_{AP}/M_P with molecular mass of the dextran is summarized in Fig. 2 for cytochrome c (○) as well as for carbonic anhydrase (●). Solid lines signify the dependence predicted by the random-flight model of the polymer [Eq. (6)], whereas the broken lines are the corresponding theoretical descriptions for dextran modelled as a rigid impenetrable sphere. As well as being more realistic physically, the random-flight model of the dextran is preferable thermodynamically in that it provides a better description of the experimental dependence of B_{AP}/M_P upon molecular mass of the dextran cosolute. Another point to note from Fig. 2 is the inverse dependence of the specific protein–polymer virial coefficient upon M_P, a result at variance with the reported independence of B_{AP}/M_P upon molecular mass deduced from gel chromatography studies [33]. However, from Fig. 2 it is evident that most of the variation in B_{AP}/M_P with molecular mass occurs in the region below 40 kDa: for longer dextran chains the specific virial coefficient becomes effectively independent of M_P. In the latter regard the predictions of the Jansons–Phillips

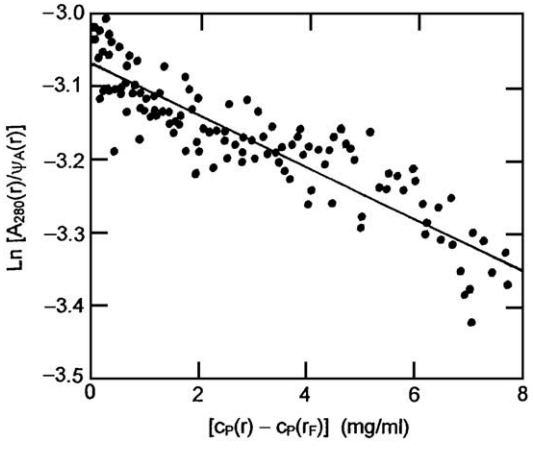

Fig. 1. Evaluation of the second virial coefficient for the excluded-volume interaction between carbonic anhydrase and dextran T20 by sedimentation equilibrium. Results from spectrophotometric (A_{280}) and Rayleigh records of the equilibrium distribution at 14,000 rpm and 20 °C are plotted in accordance with Eq. (5).

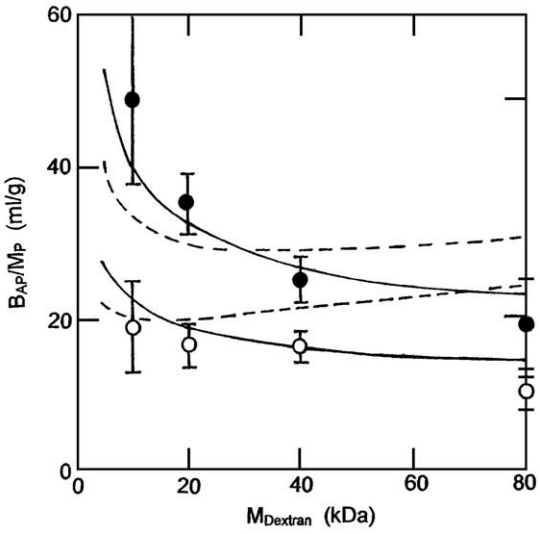

Fig. 2. Effect of polymer molecular mass on the specific second virial coefficient (B_{AP}/M_P) for the excluded-volume interactions between proteins and dextrans: (●) carbonic anhydrase; (○) cytochrome c. Solid lines denote the dependencies predicted by the Brownian walk model [17] of the polymer [Eq. (6)], whereas the broken lines are the corresponding relationships for dextran modelled as a sphere [Eq. (7)].

treatment [17] thus emulate those based on long-rod [15] and flexible segment [16,35] models of the polymer; and also conform with the experimental observations [33], which only referred to dextrans with molecular masses in the range 70–2000 kDa.

3.2. Dependence of B_{AP}/M_P upon the molecular mass of polyethylene glycol

The dependence of the virial coefficient for protein–polymer interaction upon the molecular mass of polyethylene glycol has been examined for human serum albumin by Atha and Ingham [29], who employed protein solubility measurements for virial coefficient estimation. Whereas essentially identical estimates of the specific protein–polymer virial coefficient were obtained with PEG-20000 and PEG-8000 as cosolute, the values exhibited a systematic decrease with further decrease in size of the polymer (○, Fig. 3). Such behaviour is certainly inconsistent with predictions of the random-flight (—) and spherical (- - -) models for polyethylene glycol, which essentially coincide over this range of M_P. On the other hand the virial coefficient estimate of 210 ml/g for PEG-1000 (●) obtained by equilibrium dialysis [29] conforms with theoretical prediction, as does the value of 58 (±4) ml/g for PEG-20000 (♦) that is inferred from our earlier gel chromatographic and sedimentation equilibrium study of protein–polymer interactions [20]. In view of the seven-fold discrepancy between the estimates of B_{AP}/M_P obtained from dialysis and solubility measurements of the albumin–PEG-1000 interaction [28], the merits of the two approaches deserve further investigation.

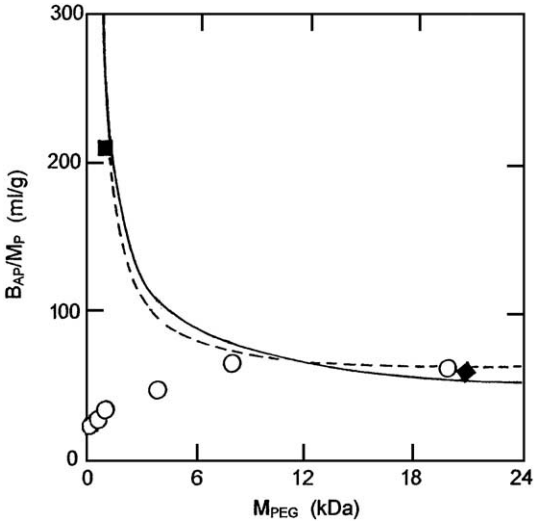

Fig. 3. Effect of polymer molecular mass on the specific second virial coefficient (B_{AP}/M_P) for the protein–polymer interaction between human serum albumin and polyethylene glycol obtained from protein solubility (○) and equilibrium dialysis (■) measurements by Atha and Ingham [29]. The solid and broken lines denote the respective dependencies predicted by the Brownian walk [Eq. (6)] and spherical [Eq. (7)] models of the polymer for a protein with R_A=3.5 nm. ♦, value for the albumin–PEG-20000 interaction inferred from [20].

The equilibrium dialysis method takes advantage of the identity of the chemical potentials of the PEG-1000 in the protein (α) and diffusate (β) phases, a situation which leads to the expression [29]

$$\ln\left(C_P^{\alpha}/C_P^{\beta}\right) = 2B_{PP}\left(C_P^{\beta} - C_P^{\alpha}\right) - B_{AP}C_A^{\alpha} \tag{9}$$

where B_{PP} is the second virial coefficient for polymer self-interaction. By using tritium-labelled polyethylene glycol, C_P^{β} was rendered sufficiently small (20–70 μM) for the self-interaction term in Eq. (9) to be effectively zero. Consequently, B_{AP} could be obtained from the slope of the dependence of $\ln(C_P^{\alpha}/C_P^{\beta})$ upon albumin concentration C_A^{α} [29]. The value of 210 ml/g for B_{AP}/M_P that is obtained from that linear dependence (see Fig. 8 of [29]) is a thermodynamically rigorous estimate of the second virial coefficient for the albumin–PEG-1000 interaction.

A similar rationale applies to the determination of protein–polymer virial coefficients from solubility measurements, which also entail phase separation. The presence of excess albumin as solid phase allows the chemical potential of the protein in all saturated solutions to be identified with that of albumin in the solid state. On those grounds the counterpart of Eq. (9) was written [29] as

$$\ln(C_A^*)_P = \ln(C_A^*)_0 + 2B_{AA}\left[(C_A^*)_0 - (C_A^*)_P\right] - B_{AP}C_P \tag{10}$$

where the star superscript denotes a saturated solution and the P subscript denotes a solubility measurement in the presence of a molar concentration C_P of polymer. $(C_A^*)_0$ refers to the solubility of albumin in the absence of polymer, and B_{AA} is the second virial coefficient for albumin self-interaction. By making the approximation that $(C_A^*)_0 \gg (C_A^*)_P$, Atha and Ingham [29] based their estimates of virial coefficients upon the slope ($-B_{AP}/M_P$) of essentially linear dependencies of $\ln(c_A^*)_P$ upon c_P. However, two aspects of that analysis deserve closer scrutiny—the choice of concentration scale and the validity of the approximation entailed in Eq. (10) at the polymer concentrations employed.

Because constant temperature and pressure are the constraints under which chemical potentials are being defined, the molal thermodynamic activity is the parameter being monitored [36–38]. The expression for identity of chemical potentials (μ_A) of saturated albumin solutions in the presence and absence of polymer therefore needs to be written as

$$\ln(a_A^*)_P = \left[\mu_{A,\text{solid}} - \mu_A^o\right]/(RT) = \ln(a_A^*)_0 \tag{11}$$

where $(a_A^*)_0$ refers to the molal thermodynamic activity of a saturated albumin solution in the absence of polymer; and where the corresponding activity in the presence of polymer, $(a_A^*)_P$, requires expression as a virial expansion in terms of molality, m_i, or its weight counterpart, w_i (g solute/kg solvent), of species. Although protein and polymer concentrations have been reported on a weight/volume basis (c_i) in the solubility study [29], their weight/weight counterparts (w_i) have been obtained therefrom, on the assumption that the solutions are incompressible, as

$$(w_A^*)_P = (c_A^*)_P/\left[\left\{1 - c_P\overline{v}_P - (c_A^*)_P\overline{v}_A\right\}\rho_s\right] \tag{12a}$$

$$w_P = c_P/\left[\left\{1 - c_P\overline{v}_P - (c_A^*)_P\overline{v}_A\right\}\rho_s\right] \tag{12b}$$

where the partial specific volumes of albumin and polyethylene glycol have been taken as 0.734 ml/g [39] and 0.84 ml/g [40], respectively: the solvent density (ρ_s) is assumed to be 1 g/ml.

The relatively high solubility $(w)_P$ of albumin in the presence of low polymer concentrations dictates the consideration of terms beyond that involving the second virial coefficient [cf, Eq. (10)] in the expansion of $\ln(a)_P$ as a function of concentration. We therefore write the left-hand side of Eq. (11) as

$$\begin{aligned}\ln(M_A a_A^*)_P = {} & \ln(w_A^*)_P + 2(C_{AA}/M_A)(w_A^*)_P \\ & + (3/2)\left(C_{AAA}/M_A^2\right)(w_A^*)_P^2 \\ & + \left[(C_{AP}/M_P) + C_{AAP}(w_A^*)_P/(M_A M_P) + \ldots\right]w_P \\ & + \left[C_{APP}/\left(2M_P^2\right) + \ldots\right]w_P^2 + \ldots\end{aligned} \tag{13}$$

in which C_{AA}, C_{AAA}, C_{AP}, etc., are the molal counterparts of the corresponding osmotic virial coefficients for a multicomponent solution. For incompressible solutions molal and

osmotic virial coefficients are related by the expressions [38]

$$C_{AA}/\rho_s = B_{AA} - M_A\overline{v}_A \tag{14a}$$

$$C_{AAA}/\rho_s^2 = B_{AAA} - (M_A\overline{v}_A)^2 \tag{14b}$$

$$C_{AP}/\rho_s = B_{AP} - (M_A\overline{v}_A + M_P\overline{v}_P)/2 \tag{14c}$$

where ρ_s is the solvent density: analytical forms expressing the third virial coefficients for protein–polymer interaction (C_{AAP}, C_{APP}) in terms of molecular shape parameters are currently unavailable. Combination of Eqs. (11) and (13) yields

$$\begin{aligned}&\ln(w_A^*)_P + 2(C_{AA}/M_A)(w_A^*)_P \\ &\quad + (3/2)\left(C_{AAA}/M_A^2\right)(w_A^*)_P^2 + \ldots \\ &\quad = \ln\left[M_A(a_A^*)_0\right] \\ &\qquad - \left[(C_{AP}/M_P) + C_{AAP}(w_A^*)_P/(M_AM_P) + \ldots\right]w_P \\ &\qquad - \left[C_{AAP}/\left(2M_P^2\right) + \ldots\right]w_P^2 + \ldots\end{aligned} \tag{15}$$

as the form of the dependence of $(w_A^*)_P$ upon polymer concentration w_P. Because of high albumin solubility, the earlier decision [29] to neglect thermodynamic nonideality arising from self-interaction of the saturated albumin solution in the presence of polymer is unjustified. Upon noting that the left-hand side of Eq. (15) represents the logarithm of the activity for an unsaturated solution of protein (no polymer present) with concentration $w_A=(w_A^*)_P$

$$\begin{aligned}\ln(M_A\alpha_A) &= \ln(w_A) + 2(C_{AA}/M_A)w_A \\ &\quad + (3/2)\left(C_{AAA}/M_A^2\right)w_A^2 + \ldots\end{aligned} \tag{16}$$

we observe that consideration of the limiting slope of the dependence of ln (M_Aa_A) upon w_P as C_{AP}/M_P requires neglect of the $C_{AAP}(w_A^*)_P/(M_AM_P)$ contribution.

For this application of the above theory the conduct of albumin solubility measurements under essentially isoelectric conditions [29] allows B_{AA} to be assigned a magnitude of 432 l/mol ($16\pi NR_A^3/3$ with R_A=3.5 nm), and advantage to be taken of the hard-sphere relationship $B_{AAA}=(5/8)B_{AA}^2$ to calculate the third osmotic virial coefficient for self-interaction of serum albumin. Although expressions are available for higher-order virial coefficients for self-interaction (B_{AAAA}, etc.), truncation of the left-hand side at the quadratic term in albumin concentration suffices for its description (maximum error of 0.2%) over the concentration range of the published solubility measurements [29]. The most extensive set of data for the current analysis refers to the protein–polymer interaction between albumin and PEG-4000 (Fig. 1 of [29]). In contrast with the essentially linear dependence of $\ln(c_A)_P$ upon c_P exhibited therein, the corresponding plot of the results according to Eq. (15) [with its left-hand side denoted as $\ln(M_Aa_A)$] is decidedly curvilinear (●, Fig. 4). Any attempt to draw a limiting tangent is obviously futile. Evaluation of second virial coefficients for albumin interactions with the other polyethylene glycols (open symbols, Fig. 4) is also clearly ruled out by the absence of data in the requisite concentration region for definition of a limiting slope.

As well as negating the earlier experimental estimates of B_{AP} for the albumin–polyethylene glycol interaction, the above considerations serve to emphasize that the use of protein solubility measurements for determining the protein–polymer second virial coefficient is restricted to relatively insoluble proteins in the presence of small concentrations of polymer (w_P<20 g/l)—the combination of circumstances which allows Eq. (15) to be simplified to

$$\ln(w_A^*)_P \approx \ln(w_A^*)_0 - (C_{AP}/M_P)w_P \tag{17}$$

which is the expression used for evaluating protein–polymer coefficients by this means and is essentially the simplified version of Eq. (10) used in [29]. In that regard albumin solubilities as high as 103 mg/ml (Fig. 3 of [29]) could not be regarded as negligible from the viewpoint of self-interaction contributions to protein nonideality; and the high polyethylene glycol concentrations (60–450 mg/ml) clearly precluded restriction of nonideality considerations to nearest-neighbour (second virial coefficient) effects. The source of the noted discrepancy [29] between estimates of B_{AP}/M_P for the albumin–PEG-1000 interaction from equilibrium dialysis and solubility measurements is thus resolved—the latter value is incorrect.

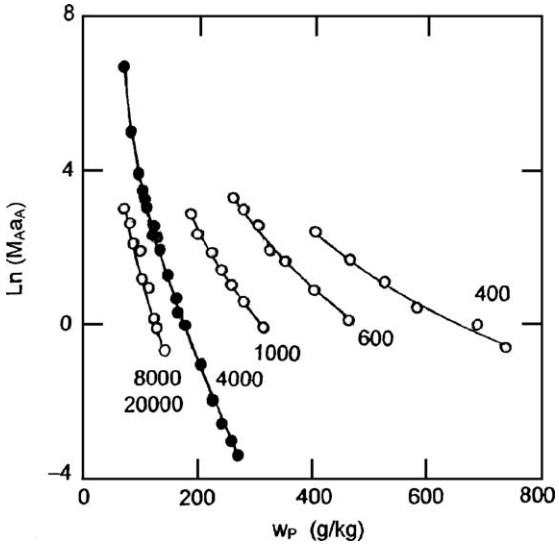

Fig. 4. Attempted evaluation of the second virial coefficient for the interaction between human serum albumin and polyethylene glycol from protein solubility measurements. The experimental data, taken from Ref. [29], are plotted according to Eq. (15) with its left-hand side denoted as ln (M_Aa_A)—see Eq. (16).

On the basis of the results presented in Fig. 3 we consider that the inverse dependence of B_{AP}/M_P upon polymer molecular mass predicted by the Jansons–Phillips treatment [17] does, indeed, describe the excluded-volume interaction between human serum albumin and polyethylene glycol. However, that conclusion does not call into question the experimental observations [29,41,42] that the effect of a given concentration of polyethylene glycol increases with increasing size of the polymeric cosolute. Instead, it again draws attention to the fact that excluded volume is not the sole determinant of the consequences of protein–polymer interaction because of the potential for involvement of the ($-CH_2CH_2-0-$) ethylene oxide repeat unit in hydrogen bonding as well as hydrophobic interaction [1,40–45]. The greater effectiveness of larger polyethylene glycols as protein precipitants reflect the chainlength dependence of this chemical reactivity—not that of excluded volume effects.

3.3. Predicted effects of polyethylene glycol size on protein equilibria

Having established that an inverse dependence upon polymer chainlength applies to the specific protein–polymer virial coefficient (B_{AP}/M_P) for a single protein species A, we now investigate the predicted effect of polyethylene glycol size on several types of macromolecular interaction. For the general equilibrium reaction $nA+B \leftrightarrows C$ the thermodynamic association constant K is given by

$$K = z_C/\left(z_A^n z_B\right) = \left[C_C/\left(C_A^n C_B\right)\right]\left[\gamma_C/\left(\gamma_A^n \gamma_B\right)\right] \quad (18)$$

where z_i denotes the molar thermodynamic activity and $\gamma_i = z_i/C_i$ the molar activity coefficient of species i. On the grounds that the equilibrium constant measured experimentally (K_{app}) is the ratio of molar concentrations raised to appropriate powers, Eq. (18) may be written as

$$K_{app}/K = \left(\gamma_A^n \gamma_B/\gamma_C\right) \quad (19)$$

which signifies that the molecular crowding effect of a cosolute such as polyethylene glycol is governed by the ratio of activity coefficients raised to the appropriate powers.

The activity coefficient of species i is related to the composition of the reaction mixture by the expression

$$\gamma_i = \exp\left[2B_{ii}C_i + \sum_{j\neq i} B_{ij}C_j + \ldots\right] \quad (20)$$

where the summation terms includes the space-filling cosolute as well as the other two reacting species. For present purposes it is considered that the concentrations of all protein species are sufficiently small for γ_i to be dominated by the protein–cosolute term, whereupon Eq. (19) can be converted to the form

$$\ln\left(K_{app}/K\right) = \left(nB_{AP} + B_{BP} - B_{CP}\right)c_P/M_P + \ldots \quad (21)$$

Predicting the effect of polymer chainlength (or M_P) for a fixed weight-concentration c_P of polyethylene glycol upon the protein reaction thus amounts to determining the effect of polymer size on $(nB_{AP}+B_{BP}-B_{CP})/M_P$; i.e., upon the appropriate difference in protein–polymer virial coefficients.

For a protein isomerization reaction $A \leftrightarrows C$ [$n=1$ and no B in Eq. (21)] we need to assess the effect of polyethylene glycol size on the magnitude of $(B_{AP}-B_{CP})/M_P$. Results of calculations based on the Jansons–Phillips model [17] with $R_A=5.2$ nm and $R_C=5.0$ nm are presented in Fig. 5, these radii being relevant to the two isomeric states of rabbit muscle pyruvate kinase [6,10]. Inverse dependencies of $(B_{AP}-B_{CP})/M_P$ upon molecular size of the polyethylene glycol are also calculated when radii pertinent to α-chymotrypsin [7], adenosine deaminase [8] and thrombin [9] isomerization are substituted for R_A and R_C (data not shown). The inference in those studies [6–10] that the detection of protein isomerization should be favoured by the use of small cosolutes thus also extends to molecular-crowding agents that are more appropriately modelled as linear chains.

In Fig. 6 we examine the effect of polyethylene glycol size on the relevant difference in protein–polymer virial coefficients for reversible protein dimerization ($2A \leftrightarrows C$). Initial calculations (—) were based on assumed spherical geometry for monomer and dimer ($R_C=2^{1/3}R_A$) and a monomer radius of 2.44 nm, a value that applies to α-chymotrypsin [24] or the αβ form of methaemoglobin [46]. An inverse dependence of $(2B_{AP}-B_{CP})/M_P$ upon polyethylene glycol molecular mass is again the predicted effect. However, consideration still needs to be given to the fact that the dimer would be more appropriately modelled as a prolate ellipsoid of revolution with an axial ratio of 2. Because the Jansons–Phillips treatment [17] models protein species as spheres, we require a magnitude for the increased

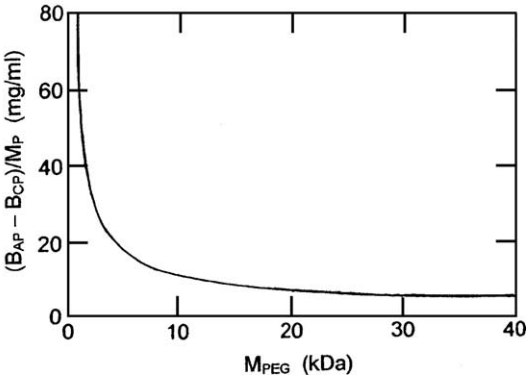

Fig. 5. Calculated effect of polyethylene glycol size (M_P) on the difference between second virial coefficients for protein–polymer interaction that governs the position of the equilibrium between the larger (A) and smaller (C) isomeric states of rabbit muscle pyruvate kinase: $K_{app}=C_C/C_A \approx K\exp[(B_{AP}-B_{CP})c_P/M_P]$. The radii of the two isomers have been taken as 5.2 and 5.0 nm, respectively [6].

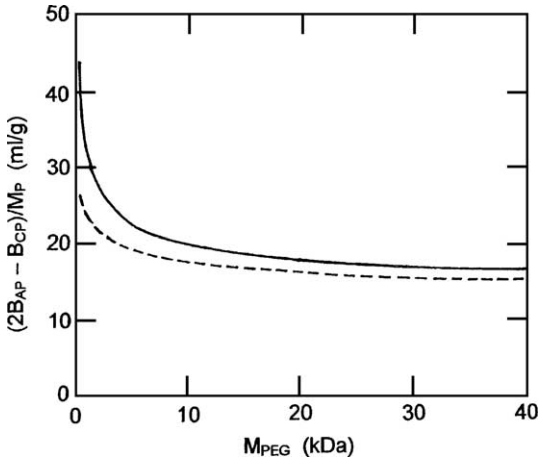

Fig. 6. Predicted effect of polyethylene glycol size (M_P) on the difference between second virial coefficients for protein–polymer interaction that governs the equilibrium position for reversible dimerization: $K_{app}=C_C/C_A^2 \approx K\exp[(2B_{AP}-B_{CP})c_P/M_P]$. Monomer (A) has been assigned a radius of 2.44 nm and dimer (C) a radius of either 3.07 nm (—) or 3.15 nm (- - -) in these calculations designed to emulate a system such as α-chymotrypsin [24] or methaemoglobin [46].

effective radius of an equivalent protein sphere that takes into account the dimer asymmetry. To obtain such a value we have taken advantage of a quantitative expression for the covolume of a spherical cosolute and a prolate ellipsoidal protein with semiaxes a_C and b_C [47,48],

$$B_{AP} = \frac{4\pi N R_P^3}{3} + \frac{4\pi N a_C b_C^2}{3} + 2\pi N a_C b_C R_P\left[\left(1-\varepsilon^2\right)^{1/2} + \left(\sin^{-1}\varepsilon\right)/\varepsilon\right] + 2\pi N a_C R_P^2\left[1 + \frac{(1-\varepsilon^2)}{2\varepsilon}\ln\frac{(1+\varepsilon)}{(1-\varepsilon)}\right] \quad (22)$$

where R_P is the cosolute radius, $\varepsilon=b_C/a_C$, a_C=2.44 nm, and b_C=4.88 nm.

On the grounds that calculations of B_{CP} on the basis of spherical geometry for dimer (R_C=3.07 nm) as well as for polyethylene glycol [Eq. (7)] yielded estimates in reasonable agreement with the Jansons–Phillips treatment [17] for $M_P \leq 6$ kDa, Eq. (22) was used to calculate the corresponding values of the protein–polymer virial coefficent for spherical cosolute and prolate ellipsoidal dimer over the same molecular mass range. Interpretation of those B_{CP} values in terms of Eq. (7) leads to an effective dimer radius of 3.15 (±0.03) nm. Incorporation of this 2.5% larger radius into the calculation of $(2B_{AP}-B_{CP})/M_P$ for the random-flight polyethylene glycol model [Eq. (6)] brings about a slight decrease in its magnitude (- - -, Fig. 6), but does not alter the prediction of an inverse dependence upon polymer chainlength.

The final situation to be considered is the effect of polymer size on the relevant covolume difference for 1:1 complex formation between dissimilar reactants, $A+B \leftrightarrows C$. For this purpose we have based the Jansons–Phillips calculations of protein–polymer virial coefficients on species radii (R_A, R_B, R_C) that should represent a reasonable approximation of the gene 45–gene 44/62 protein interaction within the T4 DNA replication complex [12]. A radius (R_A) of 3.5 nm has been assigned to the gene 45 protein (M_A=74 kDa), whereas that (R_B) of gene 44/62 protein (M_B=164 kDa) has been taken as 4.0 nm. Volume conservation considerations then lead to a radius (R_C) of 4.75 nm for the 1:1 complex modelled as a sphere. As in Fig. 6, calculation of the requisite covolume difference, $(B_{AP}+B_{BP}-B_{CP})/M_P$ in this instance, continues to yield an inverse dependence upon M_P (—, Fig. 7). That conclusion remains unaltered by employing the larger radius (R_C) that emanates from the use of Eq. (22) to model the complex as a prolate ellipsoid with semi-axes a_C=3.5+4.5=7.5 nm and b_C=(3.5+4.0)/2=3.75 nm (- - -, Fig. 7). Further increase of R_C to 4.9 nm does lead to a reversal of the molecular-size dependence for very short polymer chains (M_P<0.8 kDa), and also to prediction of the complex destabilization phenomenon [$(B_{AP}+B_{BP}-B_{CP})<0$] at low M_P first commented upon by Berg [5]. However, the form of the dependence predicted by use of this unrealistically large value for R_C (. . . . . , Fig. 7) bears little resemblance to that (●) inferred from experimental data for the effect of 10% polyethylene glycol (c_P=0.1 g/ml) on the dissociation constant k on the basis that $(B_{AP}+B_{BP}-B_{CP})/M_P=[\ln(k/k_P)]/c_P$.

On the grounds that the experimentally observed enhancement of complex formation in the presence of longer-chain polyethylene glycols [11–14] is at variance with the molecular crowding effect predicted by the most

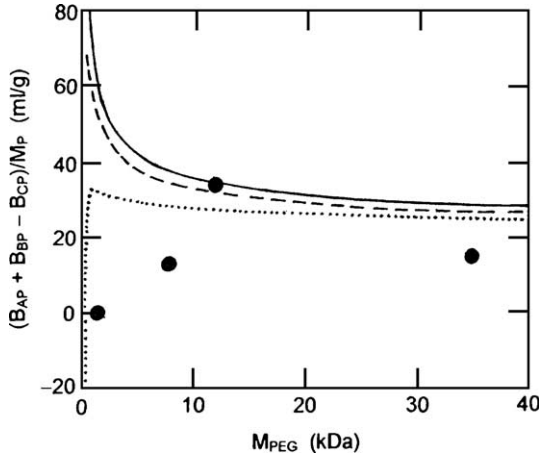

Fig. 7. Attempted theoretical descriptions of the effect of polyethylene glycol size (M_P) on reversible complex formation between the gene 45 and gene 44/62 proteins of the T4 DNA replication complex. For these calculations based on the Brownian walk model of the polymer [17] respective radii of 3.5 and 4.0 nm have been assigned to the gene 45 protein (M_A=74 kDa) and gene 44/62 protein (M_B=164 kDa). Lines refer to estimates of $(B_{AP}+B_{BP}-B_{CP})/M_P$ with the radius of the 1:1 complex (M_C=238 kDa) taken as 4.75 nm (—), 4.80 nm (- - -), and 4.90 nm (. . . . .). Circles denote experimental values of the virial coefficient difference inferred from the dissociation constants reported in Table 1 of [12].

plausible representation of excluded volume in a protein–polymer interaction [17], it again becomes necessary to invoke chemical reactivity of the space-filling cosolute as the source of the disparity between theory and experiment. The already noted propensity for noncovalent self-interaction clearly raises the spectre of weak chemical interactions between polyethylene glycol and reactant species; and hence possible changes to the magnitude of the thermodynamic association constant K. The measured equilibrium constant then becomes a weighted average of those for interaction between gene 45 and gene 44/62 proteins in native and chemically modified states. Such changes in K could well bring about the requisite decrease in B_{AP} and/or B_{PP} to reverse the dependence of $(B_{AP}+B_{BP}-B_{CP})/M_P$ upon M_P that is signified by experimental results for interactions within DNA replication complexes [11–14]. Whereas the greater enhancement of those interactions by longer-chain polyethylene glycols has previously been regarded as an excluded volume effect [12–14], the source of the phenomenon is an effect of polymer chainlength on the chemical reactivity of polyethylene glycols that overrides the corresponding consequences of excluded volume interactions.

Acknowledgements

We wish to thank Lyle E. Carrington for skilled technical assistance with the sedimentation equilibrium experimentation; and to acknowledge the delightful discussions with Professor Peter von Hippel (during a visit by DJW to the University of Oregon) that prompted this investigation.

References

[1] A.P. Minton, The effect of volume occupancy upon the thermodynamic activity of proteins: some biochemical consequences, Mol. Cell. Biochem. 55 (1983) 114–119.
[2] S.B. Zimmerman, A.P. Minton, Macromolecular crowding: biochemical and physiological consequences, Annu. Rev. Biophys. Biomol. Struct. 22 (1993) 27–65.
[3] A.P. Minton, The influence of macromolecular confinement on biochemical reactions in physiological media, J. Biol. Chem. 276 (2001) 10577–10580.
[4] W.G. McMillan, J.E. Mayer, The statistical thermodynamics of multicomponent systems, J. Chem. Phys. 13 (1945) 276–305.
[5] O.G. Berg, The influence of macromolecular crowding on thermodynamic activity: solubility and dimerization constants for spherical and dumbbell-shaped molecules in a hard-sphere mixture, Biopolymers 30 (1990) 1027–1037.
[6] S.J. Harris, D.J. Winzor, Thermodynamic nonideality as a probe of allosteric mechanisms: preexistence of the isomerization equilibrium for rabbit muscle pyruvate kinase, Arch. Biochem. Biophys. 265 (1988) 458–465.
[7] D.A. Bergman, K.E. Shearwin, D.J. Winzor, Effects of thermodynamic nonideality on the kinetics of ester hydrolysis by α-chymotrypsin: a model system with preexistence of the isomerization equilibrium, Arch. Biochem. Biophys. 274 (1989) 55–63.
[8] T.G.A. Lonhienne, D.J. Winzor, Interpretation of the reversible inhibition of adenosine deaminase by small cosolutes in terms of molecular crowding, Biochemistry 40 (2001) 9618–9622.
[9] T.G.A. Lonhienne, C.M. Jackson, D.J. Winzor, Thermodynamic nonideality as an alternative explanation of the effect of sucrose on the thrombin-catalyzed hydrolysis of peptide *p*-nitroanilide substrates, Biophys. Chemist. 103 (2003) 259–269.
[10] T.G.A. Lonhienne, P.E.B. Reilly, D.J. Winzor, Further evidence for the reliance of catalysis by rabbit muscle pyruvate kinase upon isomerization of the ternary complex between enzyme and products, Biophys. Chemist. 104 (2003) 189–198.
[11] S.B. Zimmerman, B. Harrison, Macromolecular crowding increases the binding of DNA polymerase to DNA: an adaptive effect, Proc. Natl. Acad. Sci. U. S. A. 84 (1987) 1871–1875.
[12] T.C. Jarvis, D.M. Ring, S.S. Daube, P.H. von Hippel, "Macromolecular crowding": thermodynamic consequences for protein–protein interactions within the T4 DNA replication complex, J. Biol. Chem. 265 (1990) 15160–15167.
[13] M.K. Reddy, S.E. Weitzel, P.H. von Hippel, Assembly of a functional replication complex without ATP hydrolysis: a direct interaction of bacteriophage T4 gp45 with T4 DNA polymerase, Proc. Natl. Acad. Sci. U. S. A. 90 (1993) 3211–3215.
[14] M.K. Reddy, S.E. Weitzel, S.S. Daube, T.C. Jarvis, P.H. von Hippel, Using macromolecular crowding agents to identify weak interactions within DNA replication complexes, Methods Enzymol. 262 (1995) 466–476.
[15] E. Edmond, A.G. Ogston, An approach to the study of phase separation in ternary aqueous systems, Biochem. J. 109 (1968) 569–576.
[16] J. Hermans, Excluded-volume theory of polymer–protein interactions based on polymer chain statistics, J. Chem. Phys. 77 (1982) 2193–2203.
[17] K.M. Jansons, C.G. Phillips, On the application of geometric probability theory to polymer networks and suspensions, J. Colloid Interface Sci. 137 (1990) 75–91.
[18] S. Linskog, Purification and properties of bovine erythrocyte carbonic anhydrase, Biochim. Biophys. Acta 39 (1960) 218–226.
[19] E. Margoliash, N. Frowhirt, Spectrum of horse-heart cytochrome *c*, Biochem. J. 71 (1959) 570–572.
[20] P.R. Wills, Y. Georgalis, J. Dijk, D.J. Winzor, Measurement of thermodynamic nonideality arising from volume-exclusion interactions between proteins and polymers, Biophys. Chemist. 57 (1995) 37–46.
[21] P. Voelker, Measurement of the extinction coefficient of prostatic specific antigen using interference and absorption optics in the Optima XL-A analytical ultracentrifuge, Prog. Colloid & Polym. Sci. 99 (1995) 162–166.
[22] G. Pavlov, S. Finet, K. Tatarenko, E. Korneeva, C. Ebel, Conformation of heparin studied with macromolecular hydrodynamic methods and X-ray scattering, Eur. J. Biophys. 32 (2003) 437–449.
[23] R.G. Beri, J. Walker, E.R. Reese, J.E. Rollings, Characterization of chitosans via coupled size-exclusion chromatography and multiple-angle laser light-scattering technique, Carbohydr. Res. 238 (1993) 11–26.
[24] P.R. Wills, M.P. Jacobsen, D.J. Winzor, Direct analysis of solute self-association by sedimentation equilibrium, Biopolymers 38 (1996) 119–130.
[25] J.E. Mark, P.J. Flory, The configuration of the polyoxyethylene chain, J. Am. Chem. Soc. 87 (1958) 1415–1423.
[26] K.A. Granath, Solution properties of branched dextrans, J. Colloid Sci. 13 (1958) 308–328.
[27] D.J. Winzor, L.E. Carrington, S.E. Harding, Analysis of thermodynamic nonideality in terms of protein solvation, Biophys. Chemist. 93 (2001) 231–240.
[28] S.M. Atlas, E. Farber, On the molecular weight of cytochrome *c* from mammalian heart muscle, J. Biol. Chem. 219 (1956) 31–37.

[29] D.H. Atha, K.C. Ingham, Mechanism of precipitation of proteins by polyethylene glycols: analysis in terms of excluded volume, J. Biol. Chem. 256 (1981) 12108–12117.
[30] P. DePhillips, A.M. Lentoff, Pore size distributions of cation-exchange adsorbents determined by inverse size-exclusion chromatography, J. Chromatogr., A 883 (2000) 39–54.
[31] T.C. Laurent, The interaction between polysaccharides and other macromolecules: V. The solubility of proteins in the presence of dextran, Biochem. J. 89 (1963) 253–257.
[32] T.C. Laurent, Enzyme reactions in polymer media, Eur. J. Biochem. 21 (1971) 498–506.
[33] K.E. Shearwin, D.J. Winzor, Thermodynamic nonideality in macromolecular solutions: evaluation of parameters for the prediction of covolume effects, Eur. J. Biochem. 190 (1990) 523–529.
[34] G. Rivas, J.A. Fernandez, A.P. Minton, Direct observation of the self-association of dilute proteins in the presence of inert macromolecules at high concentration via tracer sedimentation equilibrium: theory, experiment and biological significance, Biochemistry 38 (1999) 9379–9388.
[35] J.J. Hermans, J. Hermans, Distribution of polymer chainlengths inside a spherical volume: solution in terms of a diffusion problem, J. Polym. Sci., Polym. Phys. Ed. 22 (1984) 279–284.
[36] P.R. Wills, D.J. Winzor, Thermodynamic nonideality and sedimentation equilibrium, in: S.E. Harding, A.J. Rowe, J.C. Horton (Eds.), Ultracentrifugation in Biochemistry and Polymer Science, Royal Society of Chemistry, Cambridge, UK, 1992, pp. 311–330.
[37] P.R. Wills, W.D. Comper, D.J. Winzor, Thermodynamic nonideality in macromolecular solutions: interpretation of virial coefficients, Arch. Biochem. Biophys. 300 (1993) 206–212.
[38] D.J. Winzor, P.R. Wills, Thermodynamic nonideality and protein solvation, in: R.B. Gregory (Ed.), Protein–Solvent Interactions, Marcel Dekker, New York, 1995, pp. 483–520.
[39] D.J. Cox, V.N. Schumaker, The preferential hydration of proteins in concentrated salt solutions, J. Am. Chem. Soc. 83 (1961) 2433–2438.
[40] L.S. Sandell, D.A.J. Goring, Correlation between the temperature dependence of apparent specific volume and the conformation of oligomeric propylene glycols in aqueous solution, J. Polym. Sci., A-2 Polym. Phys. 9 (1971) 115–126.
[41] K.C. Ingham, Polyethylene glycol in aqueous solution: solvent perturbation and gel filtration studies, Arch. Biochem. Biophys. 184 (1977) 59–68.
[42] K.C. Ingham, Precipitation of proteins with polyethylene glycol: characterization of albumin, Arch. Biochem. Biophys. 186 (1978) 106–113.
[43] B.E. Michel, M.R. Kaufmann, The osmotic potential of polyethylene glycol 6000, Plant Physiol. 51 (1973) 914–916.
[44] D.J. Winzor, Reappraisal of disparities between osmolality estimates by freezing point depression and vapor pressure deficit methods, Biophys. Chemist. 107 (2004) 317–323.
[45] G. Tubio, B. Nerli, G. Picó, Relationship between the protein surface hydrophobicity and its partition behaviour in aqueous two-phase systems of polyethyleneglycol–dextran, J. Chromatogr., B, Biomed. Sci. Appl. 799 (2004) 293–301.
[46] M.P. Jacobsen, D.J. Winzor, Characterization of the interactions of NADH with the dimeric and tetrameric states of methaemoglobin, Biochim. Biophys. Acta 1246 (1995) 17–23.
[47] A.G. Ogston, D.J. Winzor, Treatment of thermodynamic nonideality in equilibrium studies of associating solutes, J. Phys. Chem. 79 (1975) 2496–2500.
[48] L.W. Nichol, P.D. Jeffrey, D.J. Winzor, Molecular covolumes of sphere and ellipsoid of revolution combinations, J. Phys. Chem. 80 (1976) 648–649.